

PAPER

Fabrication and characterization of SiC/Ge/graphene heterojunction with Ge micro-nano structures

To cite this article: Lianbi Li *et al* 2020 *Nanotechnology* **31** 145202

View the [article online](#) for updates and enhancements.





IOP | ebooks™

Bringing together innovative digital publishing with leading authors from the global scientific community.

Start exploring the collection—download the first chapter of every title for free.

Fabrication and characterization of SiC/Ge/graphene heterojunction with Ge micro-nano structures

Lianbi Li^{1,4,5} , Yuan Zang^{2,4} , Shenghuang Lin^{3,4}, Jichao Hu², Yuling Han², Qing Chu¹, Qianqian Lei¹ and Hong Chen¹

¹ School of Science, Xi'an Polytechnic University, Xi'an, People's Republic of China

² Department of Electronic Engineering, Xi'an University of Technology, Xi'an, People's Republic of China

³ State Key Laboratory of Applied Optics, Changchun Institute of Optics, Fine Mechanics and Physics, Chinese Academy of Sciences, Changchun, People's Republic of China

E-mail: xpu_lilianbi@163.com

Received 2 May 2019, revised 29 October 2019

Accepted for publication 31 December 2019

Published 17 January 2020



Abstract

To widen the detection wavelength range and improve the detection sensitivity of SiC-based optoelectronic devices, the SiC/Ge/graphene heterojunction was fabricated by using wet transfer of the graphene following chemical vapor deposition. The Ge films on 4H-SiC(0001) have polycrystalline structure with nano-wire (NWs) and submicron spherical island (SIs) features. Due to the distinct light trapping effect of the Ge NWs, the SiC/GeNWs/graphene heterojunction has an absorbance of more than 90% in the 500–1600 nm range, which is higher than the SiC/GeSIs/graphene heterojunction. And the SiC/GeNWs/graphene heterojunction photodetector exhibits rectification ratio up to 25 at ± 2 V and stable photoresponse to the NIR light at zero voltage bias.

Supplementary material for this article is available [online](#)

Keywords: SiC, Ge/graphene heterojunction, micro-nano structures, chemical vapor deposition

(Some figures may appear in colour only in the online journal)

1. Introduction

SiC is an optimal material for the preparation of high temperature and high power light-operated devices. However, 4H-SiC is not sensitive to most of the visible (VIS) and the entire near-infrared (NIR) spectral region, which essentially sets a limitation to its scope of optoelectronic applications [1, 2]. SiC/Ge/graphene (SiC/Ge/Gr) heterojunction proposed in this paper can be employed to widen the detection wavelength range and improve the detection sensitivity of SiC-based optoelectronic devices.

Due to the narrow bandgap (~ 0.66 eV for bulk-Ge), Ge micro-nano structures can be used as a NIR-absorption layer

in the heterojunction [1–5]. The Ge layers with micro-nano structure features can provide a large interface area for light trapping and thus enhance the NIR absorption. In recent years, in order to promote the optical absorption (OA) and photo-carriers collection, Si micro-nano structured solar cells have been extensively studied [6–9]. However, the Ge micro-nano structure photoelectrical devices on SiC are rarely reported. Due to the higher carrier mobility in Ge and the development of very good Ge/high-K dielectric interfaces, SiC/Ge hetero-diode with excellent electrical performance was prepared on 4H-SiC(0001) by using MBE method [10]. Nevertheless, the p–n heterojunction device was the traditional planar bulk form and the photoelectric characteristics of the SiC/Ge heterojunction were not investigated.

In the SiC/Ge/Gr heterojunction, the graphene has dual functions [11–17]. Due to the high optical transmittance in

⁴ These authors contributed equally to this work.

⁵ Author to whom any correspondence should be addressed.

NIR region, the graphene is an excellent electrode, which also forms a Schottky junction photodetector with Ge micro-nano structures [15]. Meanwhile, the graphene will also play an role in NIR light absorption and carrier transport [16, 17], and thereby improve the properties of the heterostructural device.

Herein, the photovoltaic SiC/Ge/Gr heterojunction with Ge micro-nano structures was constructed on 4H-SiC, and its structural and the optoelectronic properties were systematically researched. The Ge films on 4H-SiC(0001) have polycrystalline structure with nano-wire (NWs; shown in supplementary figure S1, available online at stacks.iop.org/NANO/31/145202/mmedia) and submicron spherical island (SIs; shown in supplementary figure S2) features. The heterojunction possessed rectifying characteristics and NIR photoelectric response properties at zero bias voltage. The method proposed in this paper is an effective way to realize the NIR light-operated devices with excellent high-temperature and high-power performance.

2. Experimental

The SiC/Ge/Gr heterojunctions with Ge micro-nano structures were fabricated on on-axis 4H-SiC(0001) Si-face by using wet transfer of the graphene following chemical vapor deposition [1, 2]. An n-type doped (doping concentration of 10^{17} cm^{-3}) 4H-SiC wafer with a thickness of $300 \mu\text{m}$ was purchased from II-VI Inc. Germane (GeH_4 , 5% in hydrogen) and hydrogen (H_2) were used as the source and the carrier gas respectively. The Ge micro-nano structures are grown at 750°C – 975°C for 40–100 min with a chamber pressure of $\sim 440 \text{ Pa}$. The graphene films fabrication and transfer processes are shown in details elsewhere [2]. SEM (Oxford Quanta-450), TEM (JEOL JEM-3010), Raman spectrometer (RENISHAW inVia), XRD (Rigaku Dmax-Rapid) and UV-vis spectrophotometer (Perkin Elmer, Lambda 950) were employed to determine the crystalline structure and OA spectra of the 4H-SiC/Ge/Gr heterojunctions. The OA spectra are obtained by transmission through the heterostructure at near normal incidence. The time-dependent photocurrent was measured at zero bias voltage under the illumination of 1064 nm laser (light power density: $\sim 1 \times 10^2 \mu\text{W cm}^{-2}$). The pulse laser lasts for 10 s, and the excitation turns on alternately for 10 s and off for 10 s.

3. Results and discussions

Figures 1(a), (b) show the SEM image of typical Ge self-assembled NWs on 4H-SiC(0001). The Ge NWs have high density with a diameter range of 50–300 nm. Ge nucleus is obviously observed in the cross-sectional HRTEM image, as shown in figure 1(c). The nucleus precipitates and advances upward due to the consumption of energy at the top position, afterwards it becomes fusiform and perpendicular to the 4H-SiC surface with growth time elapses. The SAED patterns at the 4H-SiC/Ge interface (figure 1(d)) can be categorized into two sets.

One has a hexagonal structure (4H-SiC[1210] zone axes) with a lattice constant of $\sim 3.08 \text{ \AA}$, which is identical to the corresponding lattice constant of the 4H-SiC. The other belongs to the Ge NWs with the polycrystalline and diamond structure.

To further clarify the crystallographic phase of the Ge micro-nano structure, XRD was employed to characterize the 4H-SiC/Ge heterojunction, as shown in figure 1(e). For the 4H-SiC/GeNWs heterojunction, the Ge NWs exhibit four main XRD peaks located at $2\theta = 27.63^\circ$, 45.81° , 54.27° and 66.24° , which belong to Ge(111), Ge(220), Ge(311) and Ge(400) planes respectively. The observation of different orientations indicates the polycrystalline structure of the Ge NWs on 4H-SiC, which verifies the SAED conclusions.

Note that the Ge NWs do not show the preferred orientation, which is different from the Ge SIs on 4H-SiC(0001). For the SiC/GeSIs heterojunction, only one XRD peak located at $2\theta = 26.68^\circ$ is observed, which proves Ge SIs on 4H-SiC have polycrystalline structure but with the preferred orientation of $\langle 111 \rangle$ [1]. The three-dimensional hetero-interface model of the 4H-SiC(0001)/Ge(111) is confirmed and depicted in figure S3. We have reported the domain matching (DM) epitaxy mode [4] of the 4H-SiC(0001)/Ge(111) heterojunction. The DM model is the standard model for the great mismatch hetero-systems such as Si/SiC [1, 2], TiN/Si [18] and GaAs/Si [19], which releases the lattice strain by the edge misfit dislocations (EMD) primarily. Based on the Ge(111)/4H-SiC(0001) interfacial structure shown in supplementary figure S3, the EMD density at the hetero-interface was calculated as $5.334 \times 10^{14} \text{ cm}^{-2}$. And the residual lattice strain (2.7% along both of the $[1120]_{4\text{H-SiC}}[011]_{\text{Ge}}$ and $[1100]_{4\text{H-SiC}}[211]_{\text{Ge}}$ orientations, shown in tabel S1) is released by the lattice relaxation. It is observed that the Ge NWs on 4H-SiC(0001) are slightly bent and arranged irregularly, which is due to the flexible characteristics of the NWs. This makes the XRD and SAED characterization results similar to those of powder samples. Even if the orientation of 4H-SiC/GeNWs heterostructure has an orientation relation of $(0001)_{4\text{H-SiC}}/(111)_{\text{Ge}}$ at the interface, the preferred orientation of GeNWs also can not be observed. Therefore, the GeNWs exhibit the polycrystalline structure without a preferred orientation, although $\langle 111 \rangle$ is the orientation with a low residual lattice stress of $\sim 2.7\%$.

The Raman spectroscopy is further performed to characterize the 4H-SiC/GeNWs heterojunction, as depicted in figure 1(f). The representative Raman spectrum is excited by a 514 nm laser. There is only one main peak located at 293.5 cm^{-1} , which correlates with Ge TO phonon mode. Note that the Raman peak of 4H-SiC is relatively weak, which is mainly due to the absorption of high density Ge NWs to the incident laser. Compared with the Ge SIs, the Raman peak of the Ge TO mode (Lorenz shape, as shown in the inset) has a red-shift (TO mode of Ge SIs is located at 297.6 cm^{-1} [1]), and the FWHM increases from 7.6 to 24.4 cm^{-1} correspondingly, confirming the decreased crystalline quality of the GeNWs.

Following the CVD fabrication of the Ge micro-nano structures on 4H-SiC, the graphene was transferred onto the

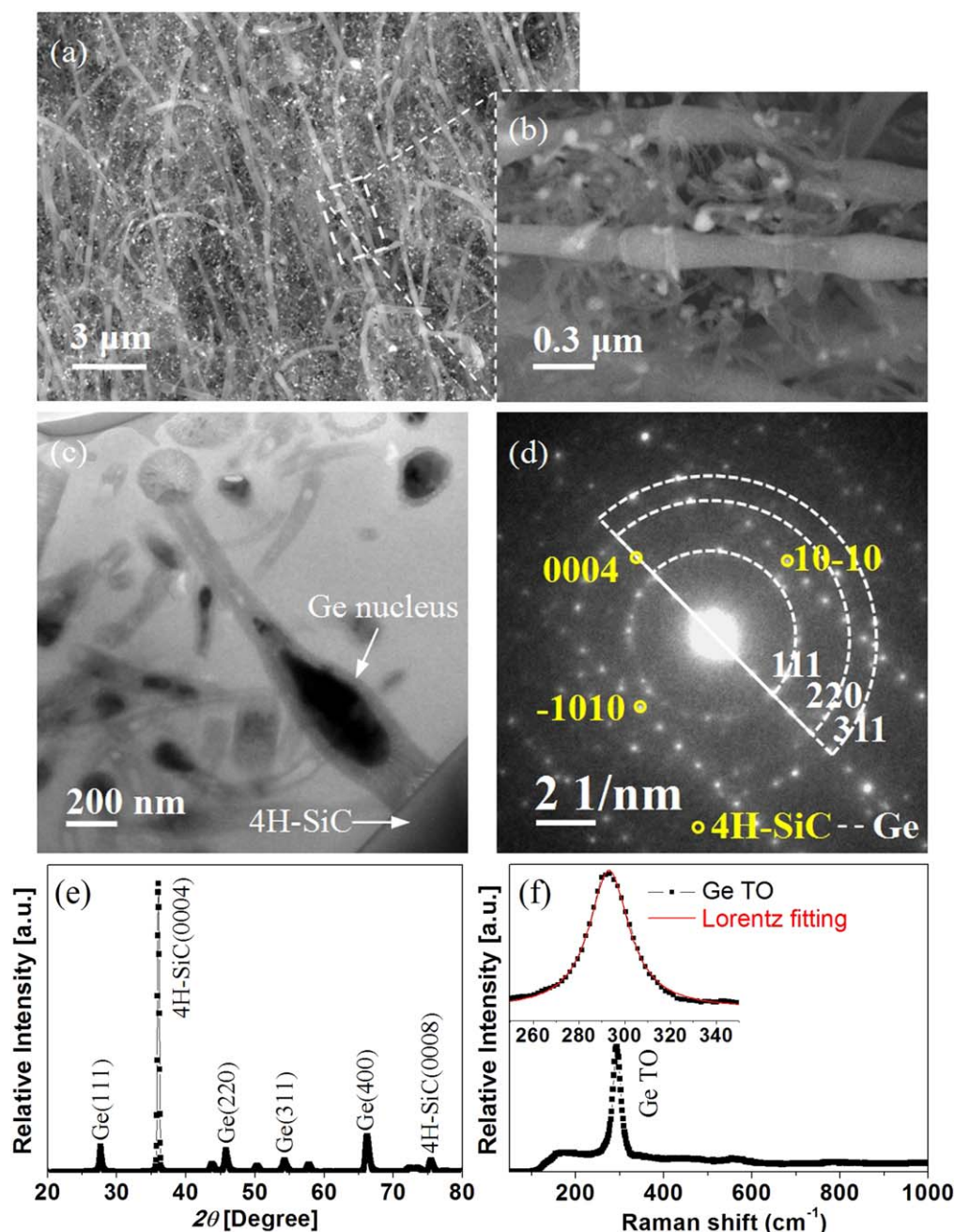


Figure 1. Characterizations of the 4H-SiC/Ge heterojunction with nano-wire features. Surface SEM images of the Ge NWs on SiC (a), (b). Cross-sectional TEM image (c) and SAED pattern (d) of the 4H-SiC/GeNWs interface corresponding to SiC[−12−10] zone axes. XRD pattern (e) and Raman spectrum (f) of the 4H-SiC/GeNWs heterojunction.

Ge micro-nano structures, despite the rough Ge surface. However, the uneven surface causes the increase of structural defects such as cracks and wrinkles, which are labeled in figure 2(a). The Raman spectra are employed to characterize the graphene layer on SiC/GeNWs heterojunction, as shown in figure 2(b). The Raman intensity ratio I_{2D}/I_G of the graphene on GeNWs is about 1.4, and the FWHM of 2D band is $\sim 46.5 \text{ cm}^{-1}$, demonstrating the transferred graphene is monolayer graphene (MLG). The D peak corresponding to the defects is still weak, signified the small amount of structural defects in MLG.

Figure 3(a) shows the schematic diagram of 4H-SiC/Ge/Gr heterojunction photodetector with Ge micro-nano structure. The diameter of the incident light spot is about $500 \mu\text{m}$, and the dimension of the region with Ge micro-nano structure is $5 \times 5 \text{ mm}^2$. The OA spectra of the SiC/Ge/Gr heterojunction (figure 3(b)) demonstrate that both of the SiC/GeNWs/Gr and SiC/GeSIs/Gr heterojunctions have the enhanced OA characteristics with an absorbance of more than 70% in the VIS–NIR band, which is conducive to the fabrication of NIR light-operated devices. Despite being only one atom thick, graphene is found to absorb a significant ($\sim 2\%$)

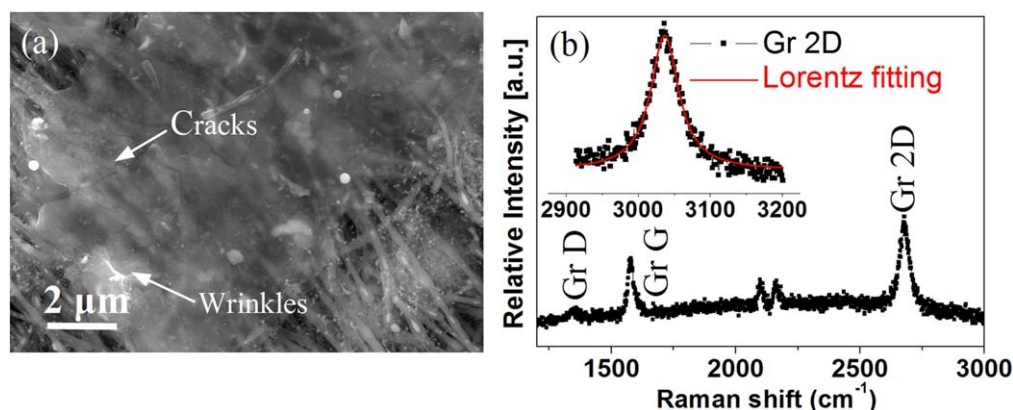


Figure 2. Surface SEM image (a) and Raman spectrum (b) of the graphene on 4H-SiC/GeNWs heterostructure. The inset shows the Raman peak of the graphene 2D mode, which is Lorentz shape with a FWHM of $\sim 46.5 \text{ cm}^{-1}$.

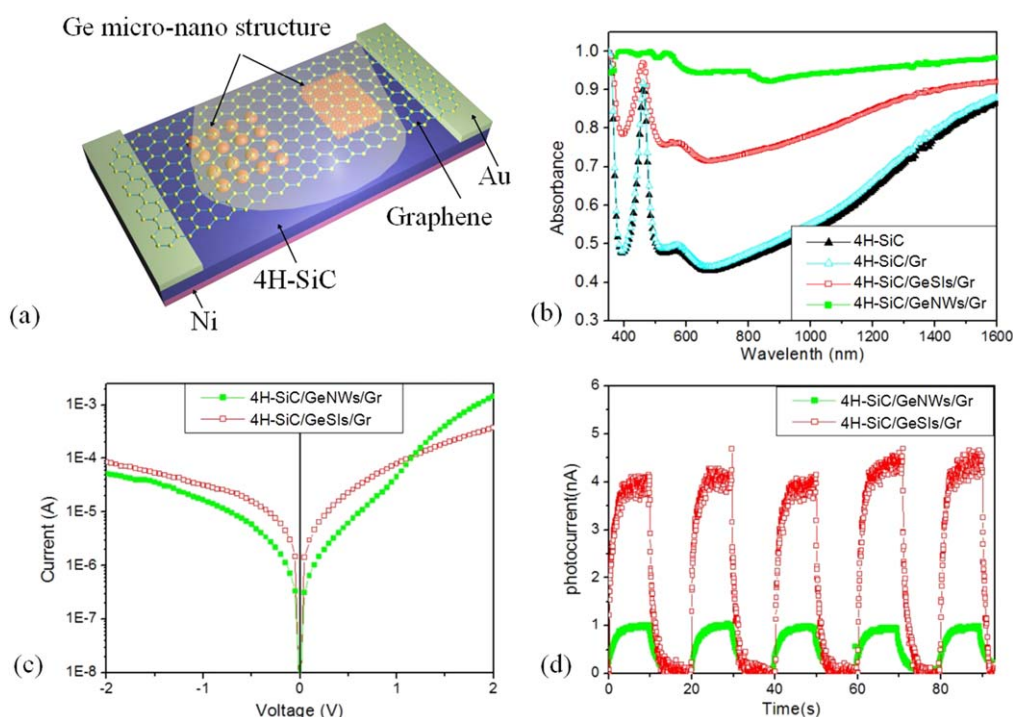


Figure 3. Schematic diagram (a), absorption spectra (b), current–voltage curves in the dark (c) and time-dependent photocurrent (d) of the 4H-SiC/Ge heterojunction photodetector with Ge micro-nano structure. The time-dependent photocurrent was measured over a 5-period on–off operation under the illumination of 1064 nm laser (light power density: $\sim 1 \times 10^2 \mu\text{W cm}^{-2}$). And the diameter of the incident light spot is $\sim 500 \mu\text{m}$.

fraction of incident VIS–NIR light, which is very close to the opacity of the MLG [20]. Note that the SiC/GeNWs/Gr heterojunction has an absorbance greater than 90%, demonstrating the distinct light trapping effect of the GeNWs. Moreover, The absorbance approaches to 100% at $\sim 368 \text{ nm}$ and $\sim 464 \text{ nm}$, which is due to the intrinsic absorption and n-type doped impurity absorption of 4H-SiC [21, 22], respectively.

Figures 3(c), (d) depict the current–voltage (I – V) curves of the SiC/Ge/Gr heterojunctions in the dark and time-dependent photocurrent under light illuminations of 1064 nm. The rectification characteristic of the SiC/GeNWs/Gr heterojunction (figure 3(c)) with a rectification ratio up to 25 at $\pm 2 \text{ V}$ can be obtained in the dark. And the reverse leakage

current at -2 V is as low as $5.18 \times 10^{-5} \text{ A}$. However, the SiC/GeSIs/Gr heterojunction has a lower rectification ratio of ~ 4.5 and higher reverse current of $8.47 \times 10^{-5} \text{ A}$. Meanwhile, the photoelectric response to pulsed 1064 nm laser illumination over a 5-period on–off operation is examined at zero voltage bias, as shown in figure 3(d). The photocurrent of the SiC/Ge/Gr heterojunctions can be effectively switched on and off while the light source is turned on and off. A steady photocurrent can be observed during the on state, which indicates that micro-nano scale heterojunctions can effectively generate and separate electron hole pairs under the NIR irradiation. Moreover, the SiC/GeNWs/Gr heterojunction has higher NIR absorbance but a lower photocurrent of $\sim 1 \text{ nA}$. It is due to the longer transportation distance of

photo-carriers, which causes the lower collection efficiency of the Gr on Ge NWs and limited the photocurrent. Moreover, the minority carrier lifetime associated with the structural defects and the doping profiles also have an impact on it. Therefore, the effects of the length and orientation of the Ge NWs on NIR-absorption and photo-carrier collection needs to be considered comprehensively. Increasing the density and shortening the length of the Ge NWs should be helpful to improve the photoelectric properties.

4. Conclusions

In this investigation, Ge NWs with the polycrystalline structure were prepared on 4H-SiC(0001) by chemical vapor deposition, and then graphene on Cu foil was wet transferred on it. The SiC/GeNWs/graphene heterostructure was prepared on 4H-SiC successfully. Due to the distinct light trapping effect of the Ge NWs, the SiC/GeNWs/graphene heterojunction has an absorbance of more than 90% in the 500–1600 nm range, which is higher than the SiC/GeSIs/graphene heterojunction. And the heterojunction photodetector exhibits rectification ratio up to 25 at ± 2 V and a steady photocurrent under NIR-irradiation at zero voltage bias.

Acknowledgments

This work was supported financially by the National Natural Science Foundation of China (Grant No. 51402230, 11975176), the Project supported by Natural Science Basic Research Plan in Shaanxi Province of China (Grant No. 2015JM6282), Scientific Research Program Funded by Shaanxi Provincial Education Department (Grant No. 14JK1302) and China Postdoctoral Science Foundation funded project (Grant No. 2013M532072).

Author contributions

Q Chu, S H Lin and Y L Han prepared the SiC/Ge/Gr heterojunction. Y Zang, J C Hu, Q Q Lei, H Chen performed XRD, Raman and TEM measurements. L B Li analyzed the data and contributes in the preparation of the manuscript.

ORCID iDs

Lianbi Li  <https://orcid.org/0000-0003-1447-1834>

Yuan Zang  <https://orcid.org/0000-0002-7854-9269>

References

- [1] Chu Q, Li L B, Zhu C J, Lin S H and Han Y L 2018 *Mater. Lett.* **211** 133–7
- [2] Han Y L, Pu H B, Zang Y and Li L B 2016 *Optoelectron. Adv. Mater.-Rapid Commun.* **10** 737–9
- [3] Kalem S, Werner P and Talalaev V 2013 *Appl. Phys. A* **112** 561–7
- [4] Yan C Y, Singh N, Cai H, Gan C L and Lee P S 2010 *ACS Appl. Mater. Interfaces* **2** 1794–7
- [5] Solanki A and Crozier K 2014 *Appl. Phys. Lett.* **105** 191115
- [6] Fan G F, Zhu H W, Wang K L, Wei J Q, Li X M, Shu Q K, Guo N and Wu D H 2011 *ACS Appl. Mater. Interfaces* **3** 721–5
- [7] Xie C et al 2011 *Appl. Phys. Lett.* **99** 133113
- [8] Yang C, Barrelet C J, Capasso F and Lieber C M 2006 *Nano Lett.* **6** 2929–34
- [9] Bae J, Kim H, Zhang X M, Dang C H, Zhang Y, Choi Y J, Nurmikko A and Wang Z L 2010 *Nanotechnology* **21** 095502
- [10] Gammon P M et al 2010 *J. Appl. Phys.* **107** 124512
- [11] Jo G et al 2010 *Nanotechnology* **21** 175201
- [12] Liu J, Yin Z, Cao X, Zhao F, Lin A P, Xie L H, Fan Q L, Boey F, Zhang H and Huang W 2010 *ACS Nano* **4** 3987–92
- [13] Seol J H et al 2010 *Science* **328** 213–6
- [14] Di C A, Wei D, Yu G, Liu Y Q, Guo Y L and Zhu D B 2010 *Adv. Mater.* **20** 3289–93
- [15] Zeng L H et al 2013 *ACS Appl. Mater. Interfaces* **5** 9362–6
- [16] Khurelbaatar Z, Kil Y H, Yun H J, Shim K H, Nam J T, Kim K S, Lee S K and Choi C J 2014 *J. Alloys Compd.* **614** 323–9
- [17] Kiraly B, Jacobberger R M, Mannix A J, Mannix A J, Campbell G P, Bedzyk M J, Arnold M S, Hersam M C and Guisinger N P 2015 *Nano Lett.* **15** 7414–20
- [18] Narayan J, Tiwari P, Chen X, Chowdhury R and Zheleva T 1992 *Appl. Phys. Lett.* **61** 1290–2
- [19] Otsuka N, Choi C, Nakamura Y, Nagakura S, Fischer R, Peng C K and Morkoç H 1986 *Appl. Phys. Lett.* **49** 277–9
- [20] Nair R R, Blake P, Grigorenko A N, Novoselov K S, Booth T J, Stauber T, Peres N M R and Geim A K 2008 *Science* **320** 1308–1308
- [21] Firsov D D, Komkov O S, Fadeev A Y and Lebedev A O 2016 *J. Phys.: Conf. Ser.* **741** 012043
- [22] Dubrowskii G B, Lepneva A A and Radovanova E I 1973 *Phys. Status Solidi b* **57** 423–31